WEST-EAST HIGH SPEED FLOW FIELD CONFERENCE
19-22, November 2007
Moscow, Russia

PREDICTION OF INCOMING TURBULENT NOISE USING A COMBINED NUMERICAL / SEMI-EMPIRICAL METHOD AND EXPERIMENTAL VALIDATION

J. Christophe*, J. Anthoine*, P. Rambaud*, C. Schram and S. Moreau*****

**von Karman Institute for Fluid Dynamics*
Chaussée de Waterloo 72, 1640 Rhode-Saint-Genèse, Belgium
E-mail: julien.christophe@vki.ac.be, anthoine@vki.ac.be, rambaud@vki.ac.be
web page: http://www.vki.ac.be
***LMS International*
Interleuvenlaan, 68 - Researchpark Z1, 3001 Leuven, Belgium
E-mail: Christophe.Schram@lmsintl.com, web page: http://www.lmsintl.com
****Valeo Thermal Systems, France*
8, rue Louis Lormand La Verrière, 78320 Le Mesnil Saint Denis, France
Email: stephane.moreau@valeo.com, web page: http://www.valeo.com

Key words: aeroacoustics, turbulent noise, airfoil, Curle's analogy, Amiet's theory, Large Eddy Simulation

Abstract. The present paper investigates the case of an airfoil placed in a turbulent jet. The Reynolds number based on the chord length is equal to 36,000 and the Mach number to 0.04. The unsteady, three-dimensional incompressible flow around the airfoil is first computed with the LES module of the commercial solver FLUENT. An innovative procedure is then proposed to compute from the CFD computation, the noise radiated for the all frequency spectrum. The SYSNOISE solver, integrating Curle's analogy limited to the computation of sound radiated by compact sources, is used to predict the low frequency part of the noise spectrum from the unsteady pressure fluctuations on the airfoil stored during the CFD flow computation. Then, Amiet's theory, specially developed for airfoil sound radiation at high frequency, is taking into account, in an explicit way, non-compactness effects. The statistical flow data, needed by Amiet's model, are fitted on the CFD data.

1. INTRODUCTION

Nowadays, flow-generated sound is a serious problem in many engineering applications. The noise pollution generated is particularly problematic in transport industry. In the aeronautics applications, the noise emitted by the landing gear, the wings and high-lift devices is a significant component of the overall noise radiated.[1-4] In automotive industry, the acoustic sound by the engine cooling and HVAC fan systems are considered as key factors in the overall appreciation of a vehicle.[5] The study and the prediction of such aerodynamic noise is all the more difficult as it involves the conversion of a very small fraction of the aerodynamic energy into acoustic energy. Among these mechanisms, unsteady turbulent interactions inside a flow and interactions of the flow with any solid boundaries play an important role. The noise emitted by the interaction of a turbulent jet with an infinite span airfoil is considered in this work.

Two different computational techniques can be used to estimate the radiated noise in the acoustic far-field: direct methods (CAA - Computational Aero-Acoustics) and indirect methods (hybrid methods). The direct approach computes the flow and sound fields altogether, which is computationally expensive. This is due to disparities between hydrodynamic and acoustic amplitudes on one side, and disparities between turbulent scales and acoustic wavelengths on the other side. The Reynolds and Mach numbers that can be achieved at reasonable computational costs by such accurate numerical approaches are hence still out of the range of practical engineering applications.

An interesting alternative is the hybrid method, in which the computation of the flow is decoupled from the computation of the sound, and consists of two steps: a) firstly, near the noise source, the flow field is obtained from an unsteady computation; b) secondly, the acoustic source radiation is computed in the far-field by the use of an analogy.[6-8] This methodology is based on the substitution of the real flow by *equivalent sources*, computed as a post-processing of the flow data. Incompressible flow modeling can be considered for the flow field at low Mach numbers, which is computationally much less involved than direct methods. Furthermore, only a restricted area around the source of noise needs to be modeled, reducing further the computational cost.

Although hybrid methods have proved their efficiency for low Helmholtz numbers – i.e. compact source regions, only few studies have indicated the numerical accuracy of the CFD modeling required to obtain good acoustic predictions and their limitations for higher frequencies (several kilohertz for our configuration).[9,10] Fine spatial and temporal discretization are needed in the flow models to sample the higher frequencies. Besides, non-compactness must be taken into account in the prediction of the acoustic field, which is usually not the case with conventional hybrid approaches.

The objective of the paper is to explore the performance of the hybrid methods at high Helmholtz numbers. This study encompasses two important aspects. On one side, we consider the optimization of important parameters of the CFD modeling with regard to the frequency range of application and computational cost. On the other side, the interpretation of the flow data as equivalent acoustical sources requires a careful discrimination between source effects and propagation effects.

This work proposes the application of such an hybrid method on the case of a turbulent round jet impacting on an infinite span airfoil. The unsteady, three-dimensional incompressible flow around the airfoil is first computed with the Large Eddy Simulation (LES) module of the commercial solver FLUENT Rev. 6.3. During the computation, the unsteady pressure data are extracted in time to be used in post-processing step for the acoustic prediction in the far field, through the SYSNOISE Rev. 5.6 solver, integrating Curle's analogy. Due to the frequency limitation of such classical hybrid method, this methodology allows us to compute the low frequency part of the noise spectrum. Besides, an innovative procedure is proposed to complement the CFD model by a semi-empirical model based on Amiet's thin-airfoil theory.[11] This theory is specially developed for airfoil sound radiation at high frequency and taking then into account non-compactness effects in an explicit way. The statistical flow data, needed by Amiet's model, are fitted on the CFD data. The Amiet's theory is then used to predict the high frequency range of the noise spectra. This methodology allows us to compute from the same CFD computation, the noise radiated for a significant frequency spectrum.

We investigate the case of a NACA0012 airfoil placed in a turbulent jet (figure 1). The nozzle outlet diameter is equal to D = 0:041 m. The airfoil is placed at zero angle of incidence and with its leading edge located at 6D from the jet outlet. The chord of the airfoil is equal to D, and the section is constant over the infinite span. The outlet

velocity magnitude U_0 is fixed to 13.2 m/s resulting in a Reynolds number based on the chord length of 36,000 and a Mach number of 0.04.

Considering this low Mach number, an incompressible flow computation is considered. Based on the characteristic dimension of the airfoil, a non-dimensional time scale $t' = tU_0/C$ is defined, where t is the physical time of the computation.

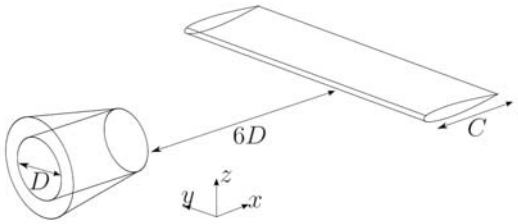

Figure 1 – Scheme of the considered geometry

2. NUMERICAL SETUP FOR FLOW COMPUTATION

The unsteady, three-dimensional incompressible flow around the airfoil is computed with the LES module of the commercial solver FLUENT Rev. 6.3. The computational domain extends to 5D in the radial direction and to 16D in the axial direction, including a 2D long nozzle before the jet outlet and a 5D long sponge zone at the end of the domain to prevent any significant reflections. The 2D long nozzle is introduced in order to have more physical and structured perturbations at the jet outlet. The flow is resolved on two different meshes of hexahedral elements and refined near the solid boundaries, around the jet and around the wing in order to reach y+ < 2 in these regions. *Case 1* has around 1 million cells while *Case 2* has around 3 millions cells. A mesh representation in the x−z plane is shown in figure 2 for *Case 2*. For both cases, the dynamic Smagorinsky type eddy viscosity is used as subgrid-scale model and second order discretization schemes are used both in space and time. A time step $\Delta t = 10^{-5}$ s is used, yielding a CFL number below 0.6 in both cases. Zero pressure condition is set at the boundaries of the domain, letting the flow coming inside the computational domain in the inlet jet plane. Inside the jet nozzle, a velocity inlet condition is imposed and tuned to reproduce Coenen's measurements performed at the von Karman Institute for Fluid Dynamics (VKI) facility described below.[12] At x = 0, corresponding to the inlet of the nozzle, the following axial velocity profile is specified:

$$u_x(r,t) = U_0\left(\frac{1}{2} - \frac{1}{2}\tanh\left(\alpha\left[\frac{r}{R_0} - \frac{R_0}{r}\right]\right)\right) \tag{1}$$

where $\alpha = 42.9$ gives the shape of the inlet profile and is based on the experimental measurements while $R_0 = D/2$.

In order to reproduce the experimental turbulence intensity at the jet outlet and to trigger the jet instability, the vortex method implemented inside FLUENT has been used for both cases. This method requires turbulent kinetic energy and energy dissipation rate profiles, which are tuned to reproduce experimental inlet conditions. A sponge zone is placed at the end of the computational domain in order to avoid numerical reflections due to the vortices crossing the downstream domain boundary, as proposed by Colonius.[13] The grid stretching acts like a filter, the large coherent structures of the flow are dissipated in smaller one, avoiding them to leave the domain with strong reflections.

Unsteady statistics (mean and RMS) are available in the whole domain for the velocity and pressure fields at a non-dimensional time $t' = 50$ for *Case 1* and $t' = 25$ for *Case 2*. The unsteady pressure data on the airfoil are stored during the same amount of time.

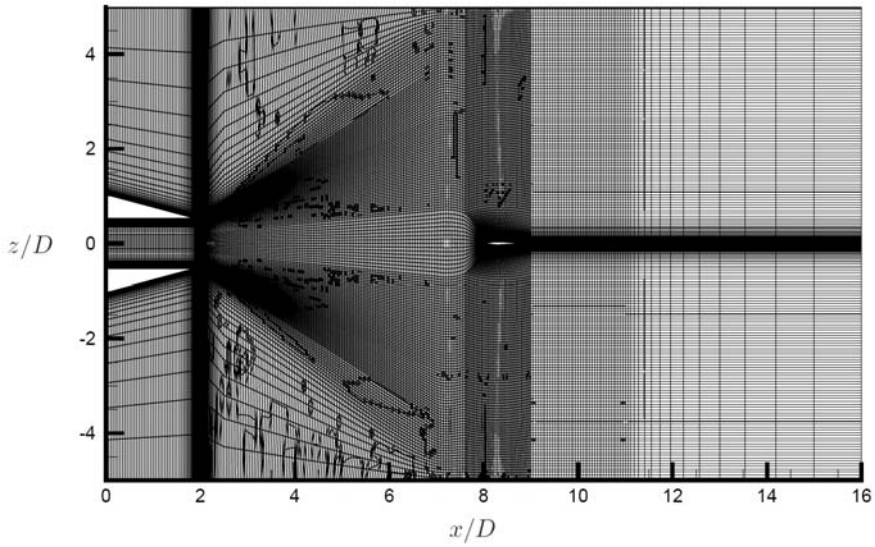

Figure 2 – Scheme of the considered geometry

3. ACOUSTIC METHODS

3.1. Curle's analogy

An aeroacoustical analogy is a reformulation of the fluid dynamic equations that allows to distinguish the sound generation mechanisms from the sound propagation. A such rearrangement of the conservation equations to obtain a single wave propagation equation was first introduced by Lighthill,[6] assuming that there are no external forces acting on the flow. Curle developed a similar analogy to take into account the noise from unsteady external forces acting on the flow; these forces being due to the presence of solid bodies into the flow.

If the viscous contribution can be neglected and if the flow is considered incompressible and isentropic, one obtains the classical result for the Curle's analogy for an impermeable and steady surface (the airfoil surface in the present case):

$$\rho'(x,t) = \frac{\partial^2}{\partial x_i \partial x_j} \iiint_V \left[\frac{T_{ij}}{4\pi c_0^2 |x-y|} \right] d^3y - \frac{\partial}{\partial x_i} \iint_{\partial V} \left[\frac{p' n_i}{4\pi c_0^2 |x-y|} \right] d^2y \qquad (2)$$

The first integral represents the incident sound field due to the aerodynamic sources distributed in the fluid volume V and the second integral represents the scattering over the boundaries ∂V of this volume. Curle's analogy considers the case of ∂V being coincident with the surface of solid bodies immersed in the unsteady flow. T_{ij} is the Lighthill's stress tensor ($T_{ij} \approx \rho_0 v_i v_j$), c_0 is the speed of sound, p' is the unsteady pressure, ρ_0 is the density in the uniform medium at rest far from the unsteady flow producing sound, v_i is the i-th velocity component.

The wall-normal viscous stresses have been neglected compared to the hydrodynamic pressure over the body surface and the bracketed terms are to be evaluated at the

retarded time $t^* = t - |x - y|/c_0$. For low Mach numbers, equivalent to the compact source assumption, an order of magnitude analysis shows that the quadrupole volume term contribution of Eq. (2), first term on right-hand side, is negligible (M^2 smaller) face to the dipolar surface integral of the same equation. It is then really attractive to neglect the quadrupolar term in order to avoid the computation of this term requiring high storage memory.

The key point of the Curle's analogy is to assume that the compressibility effects are taken into account in the flow region, including acoustic perturbations. The use of a compressible solver for the flow field computation is then an important point. The use of an incompressible solver is appropriate if the turbulence/body interaction occurs in a region that is compact enough to have minor diffraction effects. In the frame of the present work, an incompressible flow computation is considered yielding to an inappropriate use of the Curle's analogy to the high frequency range in which the source region is non-compact. This fact will be illustrated in the result section below. The unsteady pressure data on the airfoil are stored in time during the flow computation of the jet-airfoil interaction. The dipolar term from the formulation (2) is then computed in its frequency version through the acoustical solver SYSNOISE in order to compute the sound radiated in the far-field.

3.1. Simplified Amiet's theory

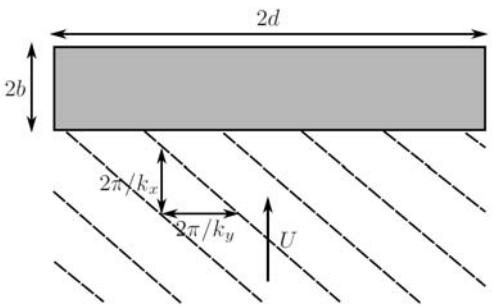

Figure 3 – Representation of a single skewed gust incident the airfoil

An airfoil of chord $2d$ and span $2b$ is placed in a turbulent fluid with a mean flow velocity U in the axial (chordwise) direction. The origin of the coordinates system is at the center of the airfoil and the observer is placed in the far-field. The turbulence is assumed to be frozen and represented in terms of its spectral wavenumber components, k_x and k_y, as illustrated in figure 3. The airfoil is assumed to be a flat plate of zero thickness, and linearized theory is considered so that the wavenumber associated with the z direction does not enter at zero angle of attack. Amiet[11] proposes an expression for the far-field acoustic PSD in terms of the turbulence energy spectrum of the upstream flow interacting with the airfoil and the airfoil response function to an incoming gust. In the large span limit and for a listener placed in the meridian plane (y = 0), only parallel gusts are considered and a simplified and approximated relation of the Amiet's theory can be written as:

$$S_{PP}(x,0,z,\omega) \cong \left(\frac{\omega z \rho_0 b}{c_0 \sigma^2}\right)^2 U \pi d \left|L(x,K_x,0)\right|^2 \Phi_{ww}(K_x,0) \tag{3}$$

where $K_x = \omega/U$, $\sigma^2 = x^2+\beta^2(y^2+x^2)$, $\beta^2 = 1-M^2$, M is the Mach number, Φ_{ww} is the two wavenumber turbulent energy spectrum for the upwash velocity component and L is the aeroacoustic transfer function, whose expression is given by Amiet.[11] This transfer function combines the unsteady aerodynamic response of the airfoil to an incident oblique gust and the corresponding acoustic propagation, and takes into account compressibility effects.

Formulation (3) give a good prediction of the far-field acoustic PSD in the case of an infinite span airfoil, for an observer placed in the mid-plane and for an

upstream turbulent flow uniform along the span. In our jet-airfoil interaction case, the last assumption is not verified. Nevertheless, this formulation (3) is used in the present work. The span is reduced to the effective span on which the jet is impacting ($y/2 = [-1; 1]$) and mean turbulent properties of the incoming flow computed on this reduced range are used as uniform input data. This procedure has the advantage to be easily usable and implementable and to give a first idea of the sound produced by a such airfoil.

4. EXPERIMENTAL SETUP

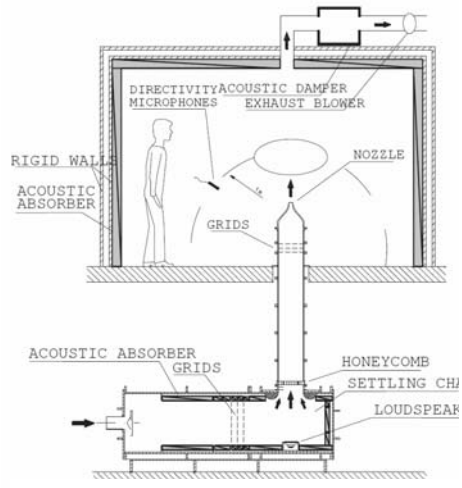

Figure 4 – Jet facility

The experimental facility, consisting in a jet discharging in a semi-anechoic room (figure 4), has been developed at the von Karman Institute for Fluid Dynamics. The dimensions of the room are 4m x 3m x 4m, and walls, ground floor and ceiling are covered with acoustic absorber. The air exhaust is acoustically insulated from outside. The cut-off frequency of the semi-anechoic room is 350Hz. The diameter of the nozzle outlet is equal to $D = 0.041$ m. The low turbulence level (below 3%) coming from the air supply, together with a high contraction ratio, allows to obtain laminar boundary layer at the outlet of the nozzle. A steel NACA0012 of 1D chord and 8.78D span is placed into the jet at a distance 6D from the jet outlet.

The velocity measurements have been obtained by hot wire anemometry. Series of 216 points were acquired with a sampling frequency of 35 kHz. Experimental velocity data are available for four profiles in the radial direction (2D, 4D, 5D and 8D) and one profile along the axial direction. Sound measurements are taken with Bruel & Kjaer microphones. A high-pass filter of 100 Hz and a low-pass filter of 12 kHz are used. The sampling frequency is 215 Hz and measurements are taken during 1 s. These measurements are available on a radius of 30 cm around the airfoil.

5. RESULTS

5.1. Experimental/numerical comparisons and flow description

Figure 5 shows a snapshot of the instantaneous flow field computed around the airfoil. The coherent structures are visualized with the second invariant of the velocity gradient tensor (Q). This criterion indicates a dominance of rotational motion in the flow when Q is positive. Since the ratio between the shear layer thickness and the jet diameter is smaller than one, the boundary layer at the nozzle exit is nearly a two-dimensional mixing layer. As the shear layer grows, it becomes three-dimensional and is dominated by the Kelvin-Helmholtz instability mechanism. These instabilities result in a roll-up of the shear-layer into vortical rings. They undergo complex three-dimensional interactions, before impinging on the airfoil. Figure 5 illustrates that the wing has a strong effect on the coherent structures deformation and that the leading edge plays a key role on this deformation. These structures either have to deviate from their original

path in order to bend away from the wing or impact on the leading edge, which tears them apart. Such reorganization of the vortical field induces pressure fluctuations on the wing surface, known as the source of the dipole sound emitted by the airfoil.[14]

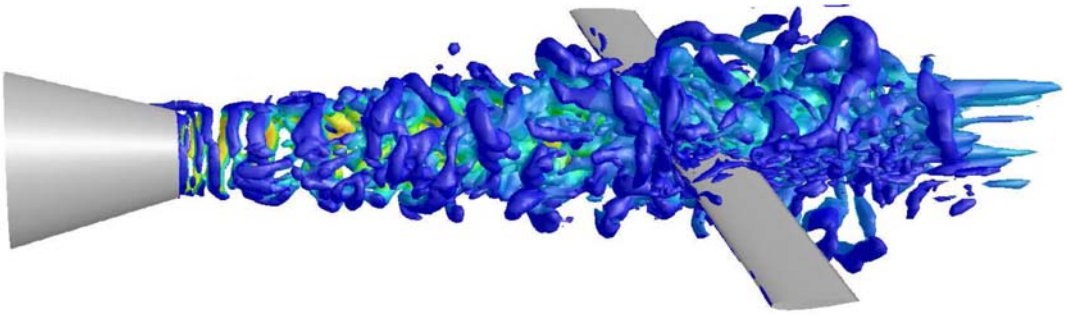

Figure 5 – Instantaneous flow field around the airfoil, coherent structures visualized with the second invariant of the velocity gradient tensor Q = 30000 colored by dynamic pressure.

Statistics of the time averaged and of the turbulent intensity based on the *x* and *z* velocity components are extracted from the unsteady LES computation and compared with experimental results in the same conditions. Transverse profiles of mean velocity magnitude and turbulence intensity are reported in figure 6 for axial positions just upstream and downstream the airfoil. The numerical transverse velocity profiles are in rather good agreement with the corresponding experimental ones. Concerning the turbulence intensity profiles, the general trend is the same between experimental and numerical results. The amplitude of turbulence intensity is different and can be probably related to the velocity inlet condition. Indeed, in the range $0 < x/D < 4$, the level of the turbulence intensity (up to 15%) is lower than the one predicted by the experiments.

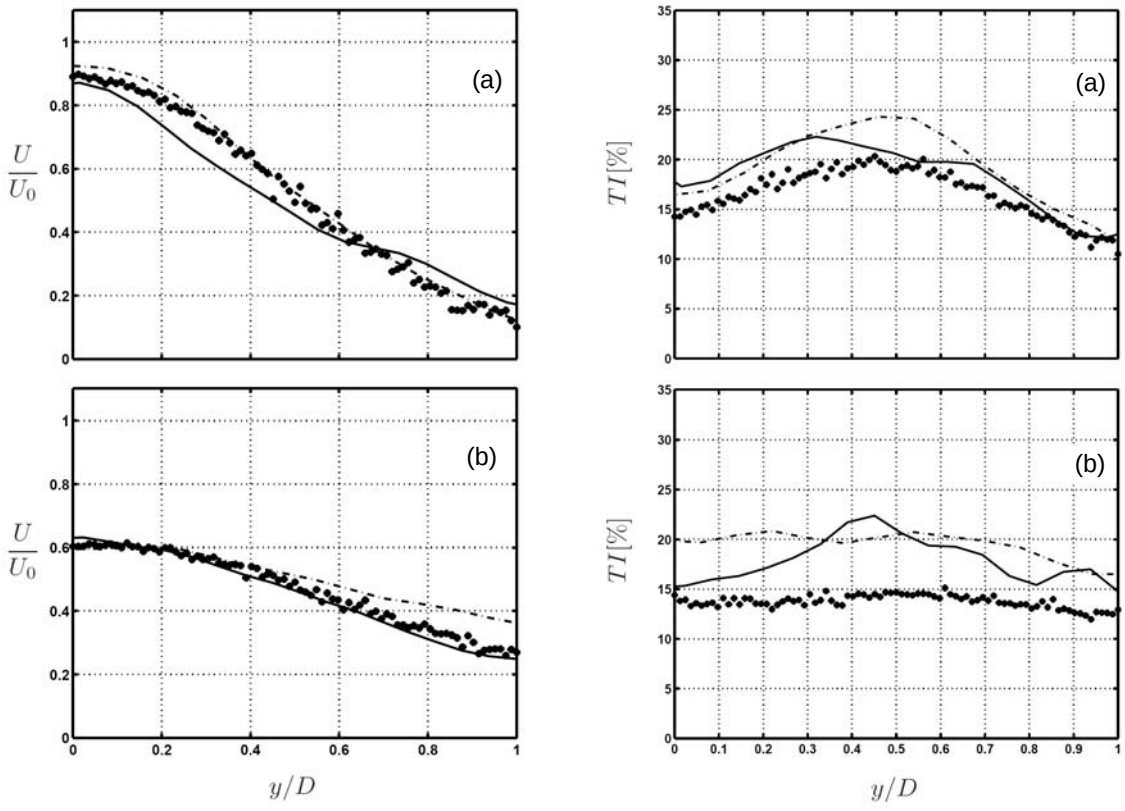

Figure 6 – Mean velocity profiles and turbulence intensity profiles, experimental (symbols) and numerical *case 1* (dash-dot) and *case 2* (plain), for $y = 5D$ (a) and $y = 8D$ (b).

This observation can be due to the numerical inlet condition that is not reproducing well the real inlet conditions or due to the mesh upstream the airfoil, having then an effect on the turbulent transition of the jet and on the over-estimation of the turbulence intensity. Even if *Case 2* is less converged in term of statistics, this case seems to present closer results compared to experiments and the fluctuations on the turbulence intensity profiles along the y axis should be damped with longer time used to obtain statistical data.

A comparison between the experimental and numerical power spectrum densities shows that the low frequency range of the power spectrum is well reproduced by the CFD computations. A cut-off frequency appears depending on the mesh refinement, 200 Hz for *Case 1* and 550 Hz for *Case 2*. As expected, the mesh refinement allows us to reach higher frequency in the frequency spectrum.

5.2. Preliminary acoustic results

As explained above, the use of the Amiet's theory requires the description of the turbulent flow upstream the airfoil with a model of turbulence in its energy spectrum. The turbulence spectra have been obtained from the CFD data stored on a 1D length upstream the airfoil and compared to the von Karman turbulence model. To obtain these spectra, the spatial correlations on the axial velocity component have been computed at the position x/D = 5.5 using interval of 1D in the axial direction centered at this point. These correlation functions have been Fourier-transformed, which yields to the turbulence energy spectra $\Phi_{uu}(k_x,0)$. Figure 7 shows that for each Fourier transformation, a turbulent scale Λ can be found in order to find the best fit compared to the von Karman model. Using a proper scaling of the abscissa using a wavenumber $k_e = (\pi^{1/2}/\Lambda)\Gamma(5/6)/\Gamma(1/3)$, all the Fourier-transformed spectra can be compared to the von Karman model on the same figure. The deviation from the von Karman model spectra shows the anisotropy of the turbulent flow upstream the airfoil. Even if the flow seems to be quite anisotropic compared to a case with uniform flow impacting an airfoil,[15] the simple model of von Karman is nevertheless chosen to describe the incoming flow turbulence. Figure 8 shows the evolution of the turbulence length Λ along the span of the airfoil in a range [−1D, 1D] around the mid-span value. The mean velocity and turbulence intensity along the span direction at x = 5.5D are represented on the same figure. The turbulence intensity and the convection speed are necessary for the use of the Amiet's theory and constant values along the span are used, corresponding to mean values of these two quantities in the range [−1D, 1D]. This preliminary procedure does not take into account the spanwise variation of the turbulence properties. The upwash turbulence spectrum has been generated using the von Karman model:

$$\Phi_{ww}(K_x,0) = \frac{4}{9\pi}\frac{\overline{u^2}}{k_e^2}\frac{\hat{k}_x^2}{\left(1+\hat{k}_x^2\right)^{\frac{7}{3}}} \tag{5}$$

where $\hat{k}_x^2 = k_x/k_e$. The velocity squared RMS $\overline{u^2}$ has been extracted from the mean value of figure 8 corresponding to a turbulence intensity of 15%. The gust convection velocity and the turbulence scale, assumed constant along the span, are respectively $0.49U_0$ and Λ = 4.51 mm.

Figure 9 shows the resulting sound pressure level computed with the Amiet's theory for an airfoil half-span d = 1D and for a listener placed at θ = 90 deg and r = 0.3 m. This procedure gives a mean effect of the all gusts interacting with the airfoil, the value obtained being too much conservative. The comparison with the experimental spectra

shows the under-prediction of the Amiet's results. This is due to the fact that the more energetic gusts are radiated predominantly on the $y = 0$ direction and have there a higher velocity than the mean one considered. Another Amiet's prediction is shown in figure 9 for which only the more energetic part of the incoming flow is considered. In this case, the airfoil half-span $d = 0.5D$ and the convection speed is $0.8U_0$, the maximum velocity at the center of the airfoil (figure 8). This time, the sound radiated is over-predicted because the convection velocity decreases in a fast way when we move away from the jet axis and is not constant along the span as considered here.

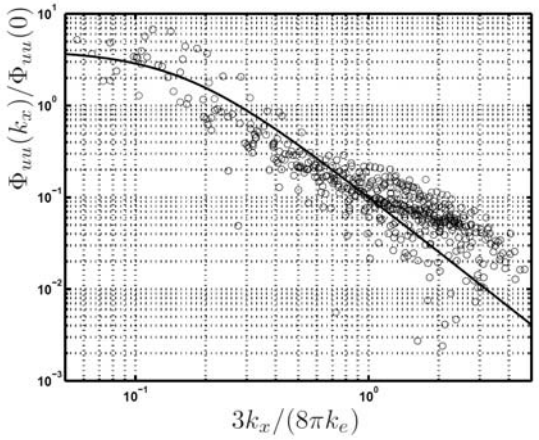

Figure 7 – Normalized axial turbulence spectrum extracted from CFD computation (o) and von Karman turbulence model (plain).

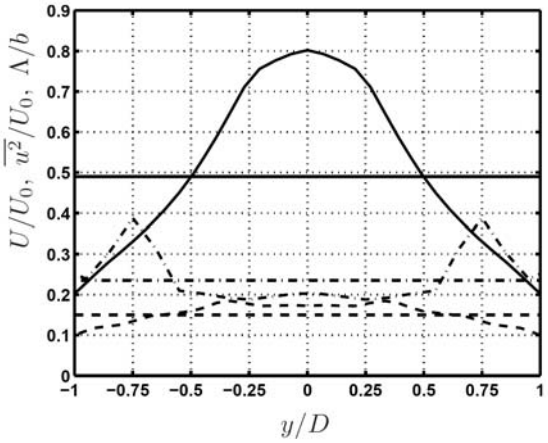

Figure 8 – Normalized mean velocity (plain), turbulence intensity (dash) and normalized turbulence scale (dash-dot) along the airfoil span and their mean value in the range $y = [-1, 1]$.

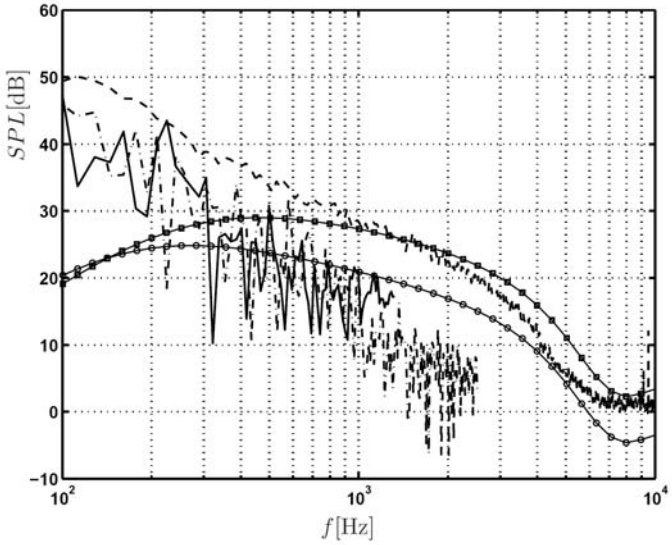

Figure 9 – SPL for an airfoil in a turbulent jet at a listener placed at $\theta = 90$ deg and $r = 0.3$ m obtained with experiments (dash), CFD *Case 1* (dash-dots), CFD *Case 2* (plain), and predicted with the Amiet's theory for a $2D$ span airfoil and $U = 0.49U_0$ (plain-square) and for a $1D$ span and $U = 0.8U_0$ (plain-circle).

Figure 9 shows also the experimental spectra, compared with the preliminary results obtained from Amiet's theory and the FLUENT/SYSNOISE procedure. It can be seen that overall, the FLUENT/SYSNOISE and Amiet predictions complement each other as anticipated, to cover the full frequency range of interest. The numerical approach covers the frequency ranges until the cut-off frequency of the CFD simulation, where Amiet's

model picks up to provide the tail of the spectrum. The agreement between the predicted and measured sound spectra is however somewhat disappointing as the FLUENT/SYSNOISE prediction stands approximately 4 to 6 dB below the measurements, even below the observed numerical cut-off frequency at about 800 Hz. Note that the comparison is irrelevant below 100 Hz, the cut-off frequency of the high-pass filter used in the acquisition loop, and that the CFD mesh refinement affects only the high frequency limit for which the sound pressure level can be computed, with a limit of 1 kHz for *Case 1* and 2 kHz for *Case 2*, the low frequency behavior being very similar.

Several factors can be invoked to explain the discrepancies between the FLUENT/SYSNOISE results and the measured spectra in the frequency range 100 Hz - 800 Hz, either bearing on experimental uncertainty/repeatability or to failures in the numerical process. These will be investigated in a systematic way. Note that if the velocity spectrum computed upstream of the airfoil shows a fair agreement with the experimental data, the pressure data itself has not been validated, while the equivalent dipoles of Curle's analogy are computed from this pressure. To the authors experience, velocity and pressure are not always computed with the same accuracy, and this could be a cause for discrepancies in the present case. The installation of unsteady pressure sensors in the airfoil is considered to permit validation of the wall pressure spectra in the future.

Anyhow, in spite of the discrepancies observed between these preliminary results, the main objective of this work is attained: it is shown that a deterministic hybrid method, specifically based in this work on Curle's analogy, can be combined with a semi-empirical method based on Amiet's theory to cover the full frequency range. The deterministic method is seen in this work to provide reasonable sound prediction up to 800 Hz for this CFD mesh size and numerical schemes used, while Amiet's theory provides the upper part of the spectrum.

6. CONCLUSION

Prelimirary results of the investigation of a round turbulent jet interacting with an airfoil have been presented. The NACA 0012 profile has the same chord than the jet diameter and is placed at 6*D* downstream the jet outlet. In a first step, the flow around the airfoil has been computed with the commercial CFD solver FLUENT. Due to the low Mach number of the flow, an incompressible 3D LES simulation has been used. The comparisons of CFD profiles at different positions in the axial direction with experimental profiles obtained in the same conditions has revealed that the velocity results are in fair agreement for the whole mean velocity field. Nevertheless, the turbulence intensity profiles have shown an over-prediction of this intensity for the numerical cases compared to the experimental one. This can be due to an unadapted inlet condition that can be improved to reach in a better way the experimental inlet conditions or/and can be due to the mesh refinement avoiding the correct development of the turbulent shear layer at the jet outlet. The influence of such parameters is still under investigation. The influence of the CFD mesh refinement has shown, as expected, the possibility to reach higher frequencies in the velocity spectrum. In a second step, the unsteady pressure data stored on the airfoil surface have been used through the SYSNOISE solver implementing the Curle's analogy. The sound prediction obtained with this FLUENT/SYSNOISE coupling exhibits a very similar slope of the spectrum, with however an overall under-prediction of about 4-6 dB in the meaningful frequency

range (100 Hz - 800 Hz). The causes of such differences are being investigated. The classical Curle's analogy is not applicable to non-compact cases when scattering effects are not taken into account by the CFD simulation. This paper has then proposed an alternative to complete the frequency spectrum with the Amiet's theory, specially developed for high frequency prediction and taking then into account the diffraction effects in a explicit way. The simplified theory used, with constant values for the flow properties along the effective span considered, has shown the applicability of such theory on the present case. Nevertheless, the use of this theory can be improved by dividing the airfoil in small segments to account for spanwise variation of the turbulence characteristics. This procedure is under implementation.

REFERENCES

[1] Perennes, S. and Roger, M., "Aerodynamic Noise of a Two-Dimensional Wing with High-Lift Devices," *AIAA Paper* 98-2338 (1998).

[2] Singer, B., Lockard, D., and Brentner, K., "Computational aeroacoustic analysis of slat trailing-edge flow," *AIAA Journal*, 38(9), 1558–1564 (2004).

[3] Brooks, T. and Humphreys Jr., W., "Flap-edge aeroacoustic measurements and predictions," *J. Sound Vib.*, 260, 31–74 (2003).

[4] Terracol, M., Labourasse, E., Manoha, E., and Sagaut, P., "Simulation of the 3D unsteady flow in a slat cove noise prediction," *AIAA Paper* 2003-3254 (2003).

[5] Caro, S. and Moreau, S., "Aeroacoustic modeling of low pressure axial flow fans," *AIAA Paper* 2000-2094 (2000).

[6] Lighthill, M., "On sound generated aerodynamically: I. General theory," *Proc. R.Soc. London Ser. A*, 211(1107), 564–587 (1952).

[7] Curle, N., "The influence of solid boundaries upon aerodynamic sound," *Proc. R.Soc. London Ser. A*, 231(1187), 505–514 (1955).

[8] Ffowcs Williams, J. and Hawkings, D., "Sound generation by turbulence and surfaces in arbitrary motions," *Proc. R.Soc. London Ser. A*, 264(1151), 321–342 (1969).

[9] Colonius, T. and Lele, S., "Computational aeroacoustics: progress on nonlinear problems of sound generation," *Progr. in Aero. Sc.*, 40(6), 345–416 (2004).

[10] Wang, M., Freund, J., and Lele, S., "Computational prediction of flow-generated sound," *Annu. Rev. Fluid Mech.*, 38, 483–512 (2006).

[11] Amiet, R., "Acoustic radiation from an airfoil in a turbulent stream," *J. Sound Vib.*, 41, 407–420 (1975).

[12] Coenen, W., "Sound emission from an airfoil in a turbulent subsonic free jet," *VKI-SR* (2005).

[13] Colonius, T., Lele, S., and Moin, P., "Boundary conditions for direct computation of aerodynamic sound generation," *AIAA Journal*, 31(9), 1574–1582 (1993).

[14] Roger, M., "Noise from moving surfaces," in *Computational Aeroacoustics, VKI Lecture Series*, 2006-05 (2006).

[15] Moreau, S., Roger, M., and Jurdic, V., "Effect of angle of attack and airfoil shape on turbulence-interaction noise," *AIAA Paper* 2005-2973 (2005).